

Heterogeneous Topology-Based Event-Triggered Consensus Control of Autonomous Motorcade Systems Against Deception Attacks

Zhou Gu [✉], Senior Member, IEEE, Jiahao Wu, Huanping Zhang, and Xiangpeng Xie [✉], Senior Member, IEEE

Abstract—This paper investigates the consensus control problem of autonomous motorcade systems with heterogeneous topology (HT) considering deception attacks. First, an HT communication method is developed to optimize the information exchange of position, velocity, and acceleration data among vehicles, thereby enhancing inter-vehicle connectivity. To alleviate the burden on the communication network, a novel HT-based event-triggered mechanism is proposed. An HT-based event-triggered control strategy is then developed for autonomous motorcade systems to counteract deception attacks. Sufficient conditions for the HT-based event-triggered autonomous motorcade tracking are derived using Lyapunov stability theory. Finally, the effectiveness and advantages of the proposed control strategy are verified through numerical simulation comparisons.

Index Terms—Autonomous motorcade systems, event-triggered mechanism, heterogeneous topology, consensus control, event-triggered mechanism.

I. INTRODUCTION

WITH the rapid growth of the global automobile industry, concerns regarding traffic congestion and driving safety have gained increased attention. Consequently, intelligent vehicle navigation and traffic scheduling have become hot topic research issues [1]. In recent years, advancements in intelligent control, wireless communication, and autonomous dispatching technologies have been employed to achieve the safe and stable unmanned motorcade travel, enhancing road traffic efficiency and optimizing transportation resource utilization [2]. Consensus control strategies are essential for autonomous motorcade systems (AMS), where multiple autonomous vehicles travel

in a single lane at predetermined spacing and speed [3], [4]. Significant progress has been achieved in the recent years, as evidenced by various studies [6], [7], [8]. For instance, in [4], master-slave formation decision-making control was studied for the AMS by using graph neural network and reinforcement learning. A state estimation-based distributed control law is developed to compensate for actuator uncertainties in the leader-follower platoon system with isomorphic network topology (INT), facilitating consensus control, as discussed in [5], [9]. Vehicle spacing and driving stability within AMS are improved by the proposed optimization techniques, enhancing road traffic throughput [6]. In [10], the consensus control of multi-agent system based on distributed adaptive feedback was designed without using global information. Despite control strategy for AMSs becoming increasingly advanced, ensuring the reliability and security of network communications remains crucial. There is an urgent need for a highly robust control strategy that can withstand cyber-attacks and operate effectively in incomplete communication networks with limited resources.

Notice that the studies mentioned above primarily focus on vehicle state information within a signal INT. However, in AMS, parameters, such as throttle opening, cylinder pressure, and coolant circulation efficiency differ among vehicles [11]. Thus, HT is more reasonable for AMS control design under these scenarios [12], [13], [14], [15]. For example, in [12], heterogeneous nonlinear systems interconnected over networks was studied for the analysis of synchronization issues, however, the design of the dynamic coupled degrees of freedom of the target is not yet conclusive. Output consensus control of heterogeneous linear systems is investigated under intermittent communication mechanisms in [13]. The study in [14] discussed heterogeneous issues of both nonlinear multi-agent systems and the communication network topologies for position and velocity interactions position and velocity interactions to achieve consensus control. The use of heterogeneous topology mitigates the impact of communication interruptions, caused by external interference or internal failures, on system performance. However, it is primarily effective for some simple systems. To the best of our knowledge, few research has focused on consensus control of AMS with heterogeneous node dynamics and network topology graphs to prevent loss of control in motorcades caused by disruptions in network connectivity between vehicles. This is one of the main motivations of this study.

Received 26 June 2024; revised 30 October 2024; accepted 21 November 2024. Date of publication 28 November 2024; date of current version 18 April 2025. This work was supported in part by the National Natural Science Foundation of China under Grant 62273183 and Grant 62103193, in part by the Startup Funding of Anhui Polytechnic University under Grant 2024YQQ001, and in part by the Natural Science Foundation of Jiangsu Province of China under Grant BK20231288. The review of this article was coordinated by Prof. Shahid Mumtaz. (Corresponding authors: Zhou Gu; Xiangpeng Xie.)

Zhou Gu is with the College of Mechanical and Electronic Engineering, Nanjing Forestry University, Nanjing 210037, China, and also with the School of Electrical Engineering, Anhui Polytechnic University, Wuhu 241000, China (e-mail: gzh1808@163.com).

Jiahao Wu and Huanping Zhang are with the College of Mechanical and Electronic Engineering, Nanjing Forestry University, Nanjing 210037, China.

Xiangpeng Xie is with the Institute of Advanced Technology, Nanjing University of Posts and Telecommunications, Nanjing 210023, China (e-mail: xiexiangpeng1953@163.com).

Digital Object Identifier 10.1109/TVT.2024.3508253

Data transmission among vehicles depends on wireless networks to facilitate consensus control in autonomous mobility systems (AMS). This necessitates sufficient network bandwidth, especially for HT-based AMSs [16]. While traditional continuous signal updates or fixed period sampling schemes can yield effective consensus control performance, they often lead to significant waste of communication and computation resources [9], [17], [18]. Over recent decades, event-triggered mechanisms (ETMs) have gained widespread attention in networked systems [19], [20] and AMSs [21], [22], [23]. An event-triggered mechanism is designed based on position and orientation to reduce the transmission frequency of data over the wireless network [19]. To enhance the adaptability of ETM for data release, the authors in [20] designed a dynamic threshold approach, aiming to achieve better filter performance compared to traditional ETMs. In [22], the authors studied the stability of event-triggered AMSs equipped with unreliable vehicle-to-vehicle communication, aiming to maintain relatively small inter-vehicle distances.

The openness of wireless networks exposes them to potential malicious attacks, posing a threat to AMS reliability. Such attacks primarily include denial of service attacks [24], [25] and deception attacks [26], [27]. Deception attacks aim to disrupt AMS performance by substituting regular data with malicious data, for example, [28] investigated the security control problem of unmanned vehicles under sensor attacks. Considering deception attacks, the authors in [29] investigated the path tracking control of autonomous vehicles, and [30] memory event triggering consensus control for multiple unmanned aerial systems. However, up to now, few researchers focus on the network reliability from network topologies to tackle the issue of AMS consensus control amidst cyber-attacks.

Based on the aforementioned discussion, this paper investigates the event-triggered consensus control of AMSs under HT considering deception attacks. The primary contributions of this paper is summarized as

- 1) A novel HT among vehicles' state information, including position, velocity, and acceleration, is taken into account. Such a topology can augment the connectivity strength of autonomous motorcades, thus mitigating the impact of connection interruption on the tracking control performance of AMSs.
- 2) A new event-triggered consensus control strategy is put forward by employing the state information of AMSs under HT. Compared with the consensus controller with isomorphic communication topology, such as in [14], [31], it is resilient to certain communication interruptions or cyber-attacks, thereby enhancing the robustness of AMSs.
- 3) A specialized matrix is introduced to address the mismatch arising from the Kronecker product between topological relations and matrix entries. Leveraging such a matrix, sufficient conditions that can guarantee the AMS stability are acquired by applying Lyapunov stability theory.

The rest of this work unfolds as follows. Section II presents the motorcade system model, the ETM and the controller design under HT. Section III gives the the stability analysis of the AMSs under event-triggered control under HT. Section IV confirms the

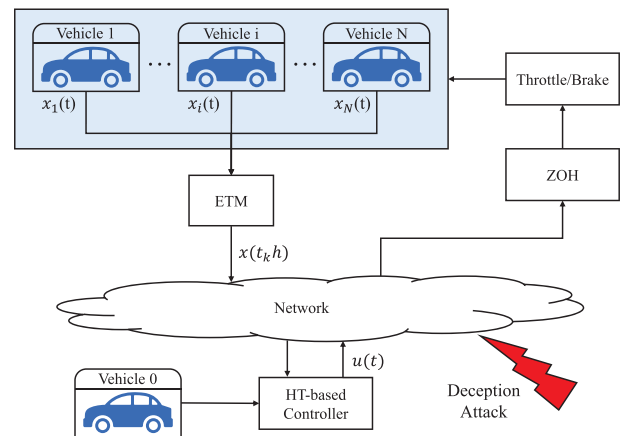


Fig. 1. Structure of AMSs with ETM.

effectiveness of the HT-based ETM via simulation examples. Finally, the conclusion of this research is drawn in Section V.

Notation: To simplify the description of the subsequent derivation in this paper, $\mathbb{E}_a = [0_{3,3(a-1)} \ I_3 \ 0_{3,3(6-a)}]$ are defined, where $a = 1, 2, \dots, 6$ and $\mathbb{E}_e = \text{col}\{\mathbb{E}_1, \mathbb{E}_2, \dots, \mathbb{E}_6\}$; $\mathbb{Q}(P|x(t)) := x^T(t)Px(t)$, and other quadratic forms are expressed in similar manner.

II. PROBLEM FORMULATION AND MODELING

The overall control structure of the AMS is shown in Fig. 1, the designed ETM determines whether to transmit vehicle status information or not. Under deception attacks, a closed-loop controller is designed based on the state information of neighbouring vehicles, which is able to avoid the interference of false packets on the stability of the AMS consensus. The subsequent sections will provide detailed explanations of each component.

A. Motorcade System Model

Consider an autonomous motorcade system, which consists of one leading vehicle and N follower vehicles traveling in a single lane. The dynamic of the i -th follower vehicle is given by [32]:

$$\dot{a}_i(t) = \chi_i(v_i, n_i, a_i, t) \quad (1)$$

with $a_i(t) = \dot{v}_i(t)$ and $v_i(t) = \dot{z}_i(t)$, where $z_i(t)$, $v_i(t)$ and $a_i(t)$ denote the position, velocity and acceleration (PVA) of vehicle i , respectively; n_i represents the engine input speed, and χ_i is governed by

$$\begin{aligned} \chi_i(v_i, n_i, a_i, t) = & -\frac{\alpha S_c d_i v_i(t) a_i(t)}{m} \\ & -\frac{1}{\iota} \left(\dot{v}_i(t) - \frac{n_i(t)}{m} + \frac{f_d}{m} + \frac{\alpha S_c d_i}{2m} v_i^2(t) \right). \end{aligned} \quad (2)$$

In (2), ι represents the time constant of the engine starting process; f_d and m are mechanical drag and mass of each vehicle, respectively; α denotes the specific mass of air; S_c is

the cross-sectional area of the vehicle under resistance, and d_i stands for the air drag coefficient.

Define the controller input that needs to be designed as $u_i(t)$, and let the engine input speed $n_i(t)$ as

$$n_i(t) = mu_i(t) + f_d + \frac{\alpha S_c d_i}{2} v_i^2(t) + \iota \alpha S_c d_i v_i(t) a_i(t). \quad (3)$$

Combining (1)–(3) follows that

$$\dot{a}_i(t) = \frac{1}{L}(u_i(t) - a_i(t)). \quad (4)$$

Inspired from [32], define the error between the i -th following vehicle and leading vehicle as $\Delta v_{i0} = v_i(t) - v_0(t)$, $\Delta a_{i0} = a_i(t) - a_0(t)$, the state error of AMS follows that

$$\begin{cases} e_z^i(t) = z_0(t) - z_i(t) - iL - z_{i0}(t) \\ e_v^i(t) = -\Delta v_{i0} \\ e_a^i(t) = -\Delta a_{i0} \end{cases}, \quad (5)$$

where L denotes the length of the vehicles; $z_{i0}(t) = \lambda_v \Delta v_{i0} + \lambda_a \Delta a_{i0} + iz_{\min}$, which represents the expected total length of the safety distance between the i -th vehicle and the leader vehicle; λ_v and λ_a are coefficients that quantify the influence of speed and acceleration on the distance, while z_{\min} refers to the minimum safe distance between vehicles.

Remark 1: Different from most of existing methods for the design of safe distance $z_{i0}(t)$ (such as in [33]), in this study, the differences of velocity and acceleration of vehicles are introduced, by which the performance of safe distance can be ensured.

Defining $x_i(t) = [e_z^i(t), e_v^i(t), e_a^i(t)]^T$ yields the tracking error system of the AMS as

$$\dot{x}_i(t) = Ax_i(t) + Bu_i(t) + D\omega_i(t), \quad (6)$$

where

$$A = \begin{bmatrix} 0 & 1 & \lambda_v - \frac{\lambda_a}{L} \\ 0 & 0 & 1 \\ 0 & 0 & -\frac{1}{L} \end{bmatrix}, B = \begin{bmatrix} -\frac{\lambda_a}{L} \\ 0 \\ -\frac{1}{L} \end{bmatrix}, D = \begin{bmatrix} \lambda_v & 0 & 0 \\ 0 & \lambda_a & 0 \\ 0 & 0 & 0 \end{bmatrix}.$$

Remark 2: A feedback linearization method is employed for the convenience of consensus control design in (6). In practice, the control input of AMSs, responsible for regulating the vehicle state, primarily relies on throttle opening that is represented by the acceleration (4). Specifically, when setting $\lambda_a = 0$, it turns to be the traditional distance model in [34].

Communication topology of all vehicles can be described by three directed weighted graphs: \mathcal{G}_z for the position, \mathcal{G}_v for the velocity, and \mathcal{G}_a for the acceleration. We take \mathcal{G}_z as an example to present graph theory of position z . For $\mathcal{G}_z = (\mathcal{P}_z, \mathcal{E}_z, \mathcal{A}_z)$, $\mathcal{P}_z = \{p_1, p_2, \dots, p_N\}$ represents the set of nodes, $\mathcal{E}_z \subseteq \mathcal{P}_z \times \mathcal{P}_z$ represents the set of directed edges, and $\mathcal{A}_z = [a_{ij}^z]_{N \times N}$ is the adjacency matrix. The directed edge e_{ij}^z is defined as the ordered pair of nodes (p_j^z, p_i^z) , and $e_{ij}^z \in \mathcal{E}_z$ if and only if $a_{ij}^z > 0$. If $e_{ij}^z \in \mathcal{E}_z$, then node j is considered a neighbor of node i , denoted as N_i^z . There exists a directed spanning tree in topology graph \mathcal{G}_z and its root node is the leading vehicle. The Laplacian matrix $L^z = [l_{ij}^z]_{N \times N}$ of the graph \mathcal{G}_z is defined as follows: $l_{ij}^z = -a_{ij}^z$ for $i \neq j$, and $l_{ii}^z = -\sum_{j=1, j \neq i}^N l_{ij}^z$. $\mathcal{G}_v = (\mathcal{P}_v, \mathcal{E}_v, \mathcal{A}_v)$

and $\mathcal{G}_a = (\mathcal{P}_a, \mathcal{E}_a, \mathcal{A}_a)$ have similar definitions of velocity and acceleration, and they are omitted here. Similarly, the pinning matrix for the position z , denoted as $B^z = \text{diag}\{b_1^z, b_2^z, \dots, b_N^z\}$, wherein $b_i^z > 0$ if the i -th vehicle is linked to the leader, otherwise $b_i^z = 0$. The matrices B^v and B^a follow the definitions to B^z .

B. A Novel Event-Triggered Mechanism

To alleviate the bandwidth overload of vehicle communication network, an ETM is proposed, wherein the instant of data transmission is determined by the designed triggering conditions rather than being fixed by the sampling period h . $t_k^i h$ is utilized to represent the k -th triggering instant of the i -th vehicle. Then, the next triggering instant is designed as follows:

$$t_{k+1}^i h = t_k^i h + \min_{\delta_i \geq 1} \{\delta_i h | \Delta(t) \leq 0\}, \quad (7)$$

where $\Delta(t) = \Sigma_1 - \Sigma_2$ and $\begin{cases} \Sigma_1 = \gamma_i + \varsigma_i(t) \bar{x}_i^T(t) \Omega_i \bar{x}_i(t) \\ \Sigma_2 = e_i^T(t) \Omega_i e_i(t) \end{cases}$, where in

$$\begin{aligned} \bar{x}_i(t) &= \sum_{j=1}^N \left\{ l_{ij} [\tilde{x}_i(t_k^i h) - \tilde{x}_j(t_k^j h)] \right\} \\ &\quad + b_i [\tilde{x}_i(t_k^i h) - \tilde{x}_0(t_k^i h + \delta_i h)], \\ \tilde{x}_0(t) &= \begin{bmatrix} z_0(t) + \lambda_v v_0(t) + \lambda_a a_0(t) \\ v_0(t) \\ a_0(t) \end{bmatrix}, \\ \tilde{x}_i(t) &= \begin{bmatrix} z_i(t) + \lambda_v v_i(t) + \lambda_a a_i(t) + iz_{\min} + iL \\ v_i(t) \\ a_i(t) \end{bmatrix}, \end{aligned}$$

and $l_{ij} = \text{diag}\{l_{ij}^z, l_{ij}^v, l_{ij}^a\}$; $t_k^i h + \delta_i h$ stands for the current sampling instant; $t_k^j h = \max\{t \in \{t_k^j h, k = 0, 1, \dots\}, t \leq t_k^i h + \delta_i h\}$ represents the j -th triggering instant; $\Omega_i > 0$ is designed as the triggering matrix; $\varsigma_i(t) = \varsigma_0 + \varsigma_m e^{-\lambda \|x_i(t_k^i h + \delta_i h)\|_2}$; and $\lambda, \varsigma_0, \varsigma_i$ and γ_i are the positive constants. Obviously, $\varsigma_0 \leq \varsigma_i(t) \leq \varsigma_0 + \varsigma_m \triangleq \hat{\varsigma}$.

Suppose the network-induced delay at instant $t_k^i h$ is $\tau_k^i \in [0, \tau_M^i]$. Then, for $t \in [t_k^i h + \tau_k^i, t_{k+1}^i h + \tau_{k+1}^i)$, we define $\tau_i(t) = t - \delta_i h - t_k^i h$. It yields that $0 < \tau_i(t) < h + \tau_M^i \leq \tau_M$, where $\tau_M = \max\{h + \tau_M^1, h + \tau_M^2, \dots, h + \tau_M^N\}$.

For convenience of description, we define

$$\beta_i(t) = \tilde{x}_i(t_k^i h + \delta_i h) - \tilde{x}_i(t_k^i h). \quad (8)$$

Thus, the $e_i(t)$ in (7) can be rewritten as

$$\begin{aligned} e_i(t) &= \sum_{j=1}^N l_{ij} [\beta_i(t_k^i h + \delta_i h) - \beta_j(t_k^j h + \delta_j h)] \\ &\quad + b_i \beta_i(t_k^i h + \delta_i h). \end{aligned} \quad (9)$$

Remark 3: In homogeneous topologies, designing consensus control is challenging due to state mismatches. To address this issue, this study constructs $\beta_i(t)$ to describe the state terms corresponding to different topological relationships.

C. Deception Attacks

Under the wireless network communication environment, vehicle state packets are vulnerable to random malicious attacks and tampering during transmission over the communication network, presenting a significant cause of disconnection in autonomous motorcade systems. Therefore, this paper considers a common network deception attack. In this scenario, we take the i -th vehicle in the motorcade as an example, an adversary randomly injects a deception signal $f_i(x_i(t))$ into the real signal $x_i(t)$ to corrupt the data packets. The real transmitted signal $\tilde{x}_i(t)$ under cyber attacks becomes

$$\tilde{x}_i(t) = \theta_i(t)f_i(x_i(t)) + (1 - \theta_i(t))\bar{x}_i(t), \quad (10)$$

where $\theta_i(t) \in \{0, 1\}$ denotes that the deception attack obeys a binomial distribution. $\bar{\theta}_i$ and κ_i^2 denote the expectation and mathematical variance of $\theta_i(t)$, respectively. When $\theta_i(t) = 0$, it indicates the absence of any attack. Conversely, $\theta_i(t) = 1$ signifies that the transmitted packet has been intercepted and manipulated by the attack signal $f_i(x_i(t))$ which is subject to the following inequality constraints:

$$\|f_i(x_i(t))\|_2 \leq \|F x_i(t)\|_2, \quad (11)$$

where $F \in \mathbb{R}^{3 \times 3}$ is a positive definition matrix.

D. Control Strategy Under HT

Given that AMSs rely on public wireless networks, the connections among vehicles are susceptible to interruptions. To enhance the robustness of the motorcade and prevent the AMS from losing control in disrupted communication scenarios, a new event-triggered control strategy under HT is developed.

Rewrite $\bar{x}_i(t)$ in (7) as

$$\bar{x}_i(t) = \begin{bmatrix} \sum_{j=1}^N l_{ij}^z \bar{z}_{ij}(t_k h) + b_i^z [\bar{z}_i(t_k^i h) - \bar{z}_0(t - \tau(t))] \\ \sum_{j=1}^N l_{ij}^v \bar{v}_{ij}(t_k h) + b_i^v [\bar{v}_i(t_k^i h) - \bar{v}_0(t - \tau(t))] \\ \sum_{j=1}^N l_{ij}^a \bar{a}_{ij}(t_k h) + b_i^a [\bar{a}_i(t_k^i h) - \bar{a}_0(t - \tau(t))] \end{bmatrix},$$

where $\bar{z}_{ij}(t_k h) = \bar{z}_i(t_k^i h) - \bar{z}_j(t_k^j h)$; velocity and acceleration follow the definition to $\bar{z}_{ij}(t_k h)$; b_i^z , b_i^v and b_i^a represent the coupling weight between the leader and the i -th vehicle in the network topology L^z , L^v and L^a , respectively.

The controller of AMSs under HT is designed by

$$\begin{aligned} u_i(t) &= -K \tilde{x}_i(t) \\ &= -K \{\theta_i(t)f_i(x_i(t)) + (1 - \theta_i(t))\bar{x}_i(t)\} \end{aligned} \quad (12)$$

for $t \in [t_k^i h + \tau_k^i, t_{k+1}^i h + \tau_{k+1}^i)$, where $K = \{K^z, K^v, K^a\}$ is the controller gain to be designed.

Remark 4: From (12), one knows that the PVA information in the control strategy has different topological relationships. Compared to the traditional control strategy, such as in [31], the connectivity and robustness of AMSs are enhanced, thereby improving the tracking performance, which is verified in the simulation in Section IV. Particularly, if one sets Laplacian matrices L^F and pinning matrices B^F be the same, e, where $r = z, v, a$ respectively; it reduces to be an INT.

To facilitate the representation, we define

$$\begin{cases} x(t) = \text{col}_{i=1}^N \{x_i(t)\}, & x(t - \tau(t)) = \text{col}_{i=1}^N \{x_i^T(t - \tau(t))\}, \\ \bar{x}(t) = \text{col}_{i=1}^N \{\text{bar}x_i^T(t)\}, & \beta(t) = \text{col}_{i=1}^N \{\beta_i^T(t)\}, \\ \omega(t) = \text{col}_{i=1}^N \{\omega_i^T(t)\}, & f(x(t)) = \text{col}_{i=1}^N \{f_i(x_i(t))\}, \\ \theta(t) = \text{diag}_{i=1}^N \{\theta_i(t)\}. \end{cases}$$

Due to the introduction of HT, it is hard to analyze and synthesize the consensus control of AMS. Accordingly, we define some new matrices E and H to address this challenge. Then, (9) can be reformulated with (8) as

$$e(t) = EHE^T \beta(t), \quad (13)$$

where $E = [\varepsilon_1 \ \varepsilon_2 \ \varepsilon_3]^T$, $\varepsilon_i = [I_i^T \ I_{i+4}^T \ I_{i+8}^T]$ and $I_i = [0_{1,i-1} \ 1 \ 0_{1,12-i}]$; $H = \text{diag}\{H^z, H^v, H^a\}$, $H^z = L^z + B^z$, H^v and H^a can be obtained identically.

Remark 5: The Laplacian matrix under traditional isomorphic topologies for AMSs, as the method in [9], can not directly match the state term of AMS. In this study, by introducing the recombination matrix E , this challenge can be elegantly addressed through the utilization of the Kronecker product.

Combining (10), (12), (13), and the ETM in (7), we can obtain the following tracking error of the AMS

$$\begin{aligned} \dot{x}(t) &= (I_N \otimes A)x(t) + \theta(t)(I_N \otimes BK)f(x(t)) \\ &\quad + (1 - \theta(t))(I_N \otimes BK)\bar{H}(x(t - \tau(t)) + \beta(t)) \\ &\quad + (I_N \otimes D)\omega(t), \end{aligned} \quad (14)$$

where $\bar{H} = E_1 H E_2$.

Remark 6: Due to the instability of wireless networks, the communication between vehicles is prone to interrupted by network congestion or malicious attacks. The weight $a_{ij} = 0$ in the adjacency matrix signifies that the i -th vehicle is not connected to the j -th vehicle.

The main objective of this study is to develop a consensus strategy for AMSs using the proposed HT-based ETM to ensure that the system (14) is ultimately uniformly bounded (UUB) in the mean-square sense.

III. CONSENSUS CONTROL DESIGN OF AMSS

In this section, some sufficient conditions to ensure the UUB stability of the motorcade error system are obtained in Theorem 1. Next, a co-design approach is formulated in Theorem 2 to get the designing parameters in (7) and (12).

Theorem 1: For given scalars τ_M , ς , r and γ , and distributed consensus controller gain K , the system (14) under HT-based ETM (7) is UUB in the mean square sense if there exist matrices $P > 0$, $Q > 0$, $\Omega > 0$, and matrix \mathcal{J}_s , such that

$$\Psi + \Gamma < 0, \quad (15)$$

$$\begin{bmatrix} \mathcal{J}_r & * \\ \mathcal{J}_s & \mathcal{J}_r \end{bmatrix} > 0, \quad (16)$$

where

$$\Psi = \Pi + 2\mathbb{E}_1 P \Phi + \Lambda, \quad \Pi = \mathbb{E}_M^T \mathcal{J} \mathbb{E}_M + \mathcal{T}^T \bar{\Omega} \mathcal{T},$$

$$\mathbb{E}_M = [\mathbb{E}_1^T \quad \mathbb{E}_2^T \quad \mathbb{E}_3^T]^T, \quad \mathcal{T} = \mathbb{E}_2 + \mathbb{E}_4, \quad \Phi = \mathcal{B}\mathbb{E}_e,$$

$$\mathcal{J} = \begin{bmatrix} -\mathcal{J}_r & * & * \\ \mathcal{J}_r + \mathcal{J}_s & -2\mathcal{J}_r - \mathcal{J}_s - \mathcal{J}_s^T & * \\ -\mathcal{J}_s & \mathcal{J}_r + \mathcal{J}_s & -\mathcal{J}_r \end{bmatrix},$$

$$\Omega = \text{diag}\{\Omega_1, \Omega_2, \dots, \Omega_N\}, \quad \bar{\Omega} = \varsigma \bar{H}^T \Omega \bar{H},$$

$$\Lambda = \text{diag}\{Q, 0, -Q, -\bar{\Omega}, 0\},$$

$$\Gamma = \tau_M^2 \Phi^T \mathcal{J}_r \Phi + \sqrt{\gamma} \mathbb{E}_1^T \mathbb{E}_1,$$

$$\mathcal{B} = [G_1 \quad (1-\theta)G_2 \quad 0 \quad (1-\theta)G_2 \quad \theta G_2 \quad G_3],$$

$$\mathcal{D} = [0 \quad \kappa G_2 \quad 0 \quad \kappa G_2 \quad -\kappa G_2 \quad 0],$$

$$G_1 = I_N \otimes A, G_2 = (I_N \otimes BK)\bar{H}, G_3 = I_N \otimes D.$$

Proof: Define $\vartheta(t) = [x(t), x(t-\tau(t)), x(t-\tau_M), \beta(t), f(x(t)), \omega(t)]$. Thus, the closed-loop tracking error of the AMS in (14) can be rewritten as

$$\dot{x}(t) = \Phi \vartheta(t). \quad (17)$$

Choose the following Lyapunov-Krasovskii functional candidate:

$$\begin{aligned} \mathcal{V}(t) = & \mathbb{Q}(P|x(t)) + \int_{t-\tau_M}^t \mathbb{Q}(Q|x(s)) ds \\ & + \tau_M \int_{t-\tau_M}^t \int_{\theta}^t \mathbb{Q}(\mathcal{J}_r|\dot{x}(s)) ds d\theta. \end{aligned} \quad (18)$$

From (11), it follows that

$$\mathcal{F} = \mathbb{Q}(P|f(x(t))) - x^T(t) \bar{F}^T P \bar{F} x(t) \leq 0, \quad (19)$$

where $\bar{F} = I_N \otimes F$.

Recalling (7), (19) and state error system (17), taking the derivative of $\mathcal{V}(t)$ yield

$$\begin{aligned} \mathcal{E}\{\dot{\mathcal{V}}(t)\} \leq & 2x^T(t) P \Phi \vartheta(t) + \tau_M^2 \mathcal{E}\{\mathbb{Q}(\mathcal{J}_r|\dot{x}(t))\} + \Delta \\ & + \mathbb{Q}(Q|x(t)) - \mathbb{Q}(Q|x(t-\tau_M)) \\ & - \tau_M \int_{t-\tau_M}^t \mathbb{Q}(\mathcal{J}_r|\dot{x}(s)) ds - \mathcal{F} \\ & - \sqrt{\gamma} x^T(t) x(t) + \sqrt{\gamma} x^T(t) x(t), \end{aligned} \quad (20)$$

where $\Delta = \mathbb{Q}(\bar{\Omega}|\zeta(t)) - \mathbb{Q}(\Omega|e(t)) + \gamma$, $\gamma = \sum_{i=1}^N \gamma_i$ and $\zeta(t) = \beta(t) + x(t-\tau(t))$.

Applying Jensen inequality [35] follows that

$$-\tau_M \int_{t-\tau_M}^t \mathbb{Q}(Q|\dot{x}(s)) ds \leq \vartheta^T(t) \mathbb{E}_M^T \mathcal{J} \mathbb{E}_M \vartheta(t). \quad (21)$$

From (7), one can know that

$$\vartheta^T(t) (-\mathbb{E}_4^T \Omega \mathbb{E}_4 + \mathcal{T}^T \bar{\Omega} \mathcal{T} + \gamma) \vartheta(t) > 0. \quad (22)$$

Combining (20), (21) and (22), one has

$$\mathcal{E}\{\dot{\mathcal{V}}(t)\} \leq \vartheta^T(t) (\Psi + \Gamma) \vartheta(t) + \gamma - \sqrt{\gamma} x^T(t) x(t). \quad (23)$$

According to $x^T(t) x(t) \geq \sqrt{\gamma}$ and the condition (15) in Theorem 1, one can obtain $\mathcal{E}\{\dot{\mathcal{V}}(t)\} < 0$, which means that the

considered AMS under the HT-based ETM is UUB in the mean-square sense. This ends the proof. ■

Theorem 2: For given scalars τ_M, ς, r and γ , the system (14) is UUB in the mean square sense if there exist positive definite matrices $\hat{P} > 0, \hat{Q} > 0, \hat{\mathcal{J}}_s > 0, \hat{\Omega} > 0$, and matrix \hat{K} such that

$$\begin{bmatrix} \hat{\Psi} & * & * \\ \tau_M \hat{\Phi} & \mu^2 \hat{\mathcal{J}}_r - 2\mu \hat{P} & * \\ \hat{\Xi} & 0 & -I \end{bmatrix} < 0, \quad (24)$$

$$\begin{bmatrix} \hat{\mathcal{J}}_r & * \\ \hat{\mathcal{J}}_s & \hat{\mathcal{J}}_r \end{bmatrix} > 0, \quad (25)$$

where

$$\hat{\Psi} = \hat{\Pi} + 2\mathbb{E}_1 \hat{\Phi} + \hat{\Lambda}, \quad \hat{\Pi} = \mathbb{E}_M^T \hat{\mathcal{J}} \mathbb{E}_M + \varsigma \mathcal{T}^T \hat{\Omega} \mathcal{T},$$

$$\mathbb{E}_M = [\mathbb{E}_1^T \quad \mathbb{E}_2^T \quad \mathbb{E}_3^T]^T, \quad \mathcal{T} = \mathbb{E}_2 + \mathbb{E}_4, \quad \hat{\Phi} = \hat{\mathcal{B}}\mathbb{E}_e,$$

$$\hat{\mathcal{J}} = \begin{bmatrix} -\hat{\mathcal{J}}_r & * & * \\ \hat{\mathcal{J}}_r + \hat{\mathcal{J}}_s & -2\hat{\mathcal{J}}_r - \hat{\mathcal{J}}_s - \hat{\mathcal{J}}_s^T & * \\ -\hat{\mathcal{J}}_s & \hat{\mathcal{J}}_r + \hat{\mathcal{J}}_s & -\hat{\mathcal{J}}_r \end{bmatrix},$$

$$\hat{\Lambda} = \text{diag}\{\hat{Q}, 0, -\hat{Q}, -\hat{\Omega}, 0\},$$

$$\hat{\Xi} = [\gamma^{0.25} \hat{P} \quad 0 \quad 0 \quad 0 \quad 0],$$

$$\hat{\mathcal{B}} = [\bar{G}_1 \quad (1-\theta)\bar{G}_2 \quad 0 \quad (1-\theta)\bar{G}_2 \quad \theta\bar{G}_2 \quad G_3],$$

$$\hat{\mathcal{D}} = [0 \quad \kappa\bar{G}_2 \quad 0 \quad \kappa\bar{G}_2 \quad -\kappa\bar{G}_2 \quad 0],$$

$$\bar{G}_1 = (I_N \otimes A)\bar{P}, \bar{G}_2 = (I_N \otimes BK)\bar{H}, G_3 = I_N \otimes D.$$

Furthermore, the proposed controller gain and the event-triggered matrix is derived as $K = \hat{K}\hat{P}_s^{-1}$ and $\Omega_i = \hat{P}_s^{-1}\hat{\Omega}_i\hat{P}_s^{-1}$, respectively.

Proof: Define $P = \bar{H}\hat{P}\bar{H}$, $\hat{P} = (I_N \otimes \hat{P}_s)$, $\hat{P}_s = \hat{P}_s^{-1}$, $\bar{P} = \hat{P}^{-1}$, $\bar{P} = P^{-1} = \bar{H}^{-1}\hat{P}\bar{H}^{-1}$, so that $\hat{Q} = \bar{P}Q\bar{P}$, $\hat{\mathcal{J}}_r = \bar{P}\mathcal{J}_r\bar{P}$, $\hat{\mathcal{J}}_s = \bar{P}\mathcal{J}_s\bar{P}$, $\hat{K} = K\hat{P}_s$, $\hat{\Omega}_i = \hat{P}_s\Omega_i\hat{P}_s$, $\hat{\Omega} = \text{diag}\{\hat{\Omega}_1, \hat{\Omega}_1, \dots, \hat{\Omega}_N\}$, $\hat{\Omega} = \bar{H}^{-T}\hat{\Omega}\bar{H}^{-1}$.

Applying Schur complement and the attribute of $-\mathcal{J}_r^{-1} = -\bar{P}\hat{\mathcal{J}}_r^{-1}\bar{P} \leq \mu^2\hat{\mathcal{J}}_r - 2\mu\bar{P}$, one can obtain from the condition (15) that

$$\begin{bmatrix} \Psi & * & * \\ \tau_M \Phi & \mu^2 \hat{\mathcal{J}}_r - 2\mu \bar{P} & * \\ \Xi & 0 & -I \end{bmatrix} < 0, \quad (26)$$

where $\Xi = [\gamma^{0.25} I \quad 0 \quad 0 \quad 0 \quad 0]$. Then, applying left-multiplication and right-multiplication with the diagonal matrices $\text{diag}\{\bar{P}, \bar{P}, \bar{P}, \bar{P}, \bar{P}, I, I, I, \bar{P}, I\}$ and $\text{diag}\{\bar{P}, \bar{P}\}$ to inequalities (26) and (16), we can obtain (27) and (28). This completes the proof. ■

As noted in Remark 4, the proposed motorcade under HT can be reduced to the conventional INT structure when the Laplacian matrices L^x and pinning matrices B^x are the same.

Corollary 1: For given scalars τ_M, ς, r and γ , the AMS (14) under the conventional INT structure is UUB in the mean

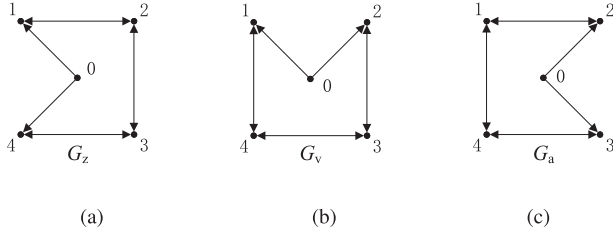


Fig. 2. The topology graph of PVA.

square sense if there exist positive definite matrices $\widehat{P}_c > 0$, $\widehat{Q}_c > 0$, $\widehat{\mathcal{J}}_{sc} > 0$, $\widehat{\Omega}_c > 0$ and matrix \widehat{K}_c such that

$$\begin{bmatrix} \widehat{\Psi}_c & * & * \\ \tau_M \widehat{\Phi}_c & \mu^2 \widehat{\mathcal{J}}_{rc} - 2\mu \widehat{P}_c & * \\ \widehat{\Xi}_c & 0 & -I \end{bmatrix} < 0, \quad (27)$$

$$\begin{bmatrix} \widehat{\mathcal{J}}_{rc} & * \\ \widehat{\mathcal{J}}_{sc} & \widehat{\mathcal{J}}_{rc} \end{bmatrix} > 0, \quad (28)$$

where

$$\widehat{\Psi}_c = \widehat{\Pi}_c + 2\mathbb{E}_1 \widehat{\Phi}_c + \widehat{\Lambda}_c, \quad \widehat{\Pi}_c = \mathbb{E}_M^T \widehat{\mathcal{J}}_c \mathbb{E}_M + \varsigma \mathcal{T}^T \widehat{\Omega}_c \mathcal{T},$$

$$\mathbb{E}_M = \begin{bmatrix} \mathbb{E}_1^T & \mathbb{E}_2^T & \mathbb{E}_3^T \end{bmatrix}^T, \quad \mathcal{T} = \mathbb{E}_2 + \mathbb{E}_4, \quad \widehat{\Phi}_c = \widehat{B}_c \mathbb{E}_e,$$

$$\widehat{\mathcal{J}}_c = \begin{bmatrix} -\widehat{\mathcal{J}}_{rc} & * & * \\ \widehat{\mathcal{J}}_{rc} + \widehat{\mathcal{J}}_{sc} & -2\widehat{\mathcal{J}}_{rc} - \widehat{\mathcal{J}}_{sc} - \widehat{\mathcal{J}}_{sc}^T & * \\ -\widehat{\mathcal{J}}_{sc} & \widehat{\mathcal{J}}_{rc} + \widehat{\mathcal{J}}_{sc} & -\widehat{\mathcal{J}}_{rc} \end{bmatrix},$$

$$\widehat{\Lambda}_c = \text{diag}\{\widehat{Q}_c, 0, -\widehat{Q}_c, -\widehat{\Omega}_c, 0\},$$

$$\widehat{\Xi}_c = [\gamma^{0.25} \widetilde{P} \quad 0 \quad 0 \quad 0 \quad 0],$$

$$\widehat{B}_c = [\widetilde{G}_1^c \quad (1-\theta)\widetilde{G}_2^c \quad 0 \quad (1-\theta)\widetilde{G}_2^c \quad \theta\widetilde{G}_2^c \quad G_3],$$

$$\widehat{D}_c = [0 \quad \kappa\widetilde{G}_2^c \quad 0 \quad \kappa\widetilde{G}_2^c \quad -\kappa\widetilde{G}_2^c \quad 0],$$

$$\widetilde{G}_1^c = (I_N \otimes A)\widetilde{P}, \quad \widetilde{G}_2^c = (H \otimes B)(I_N \otimes \widehat{K}_c),$$

where $\widehat{Q}_c = \widetilde{P}Q\widetilde{P}$, $\widehat{\mathcal{J}}_{rc} = \widetilde{P}\mathcal{J}_r\widetilde{P}$, $\widehat{\mathcal{J}}_{sc} = \widetilde{P}\mathcal{J}_s\widetilde{P}$, $\widehat{K}_c = K_c\widetilde{P}_s$, $\widehat{\Omega}_i^c = \widetilde{P}_s\Omega_i^c\widetilde{P}_s$, $\widehat{\Omega}^c = \text{diag}\{\widehat{\Omega}_1^c, \widehat{\Omega}_1^c, \dots, \widehat{\Omega}_N^c\}$. Further, the control gain is $K_c = \widehat{K}_c\widetilde{P}_s^{-1}$ and event-triggered weighting matrix is $\Omega_i^c = \widetilde{P}_s^{-1}\Omega_i^c\widetilde{P}_s^{-1}$.

Proof: The proof procedure is similar to Theorems 1 and 2. It is omitted here. ■

IV. SIMULATION

In this section, an AMS consisting of one leader vehicle and four follower vehicles is considered. The topological relationships between the positions, velocities and accelerations of these vehicles are shown in Fig. 2, from which the following Laplacian

matrices are obtained as

$$L^z = \begin{bmatrix} 1 & -1 & 0 & 0 \\ -1 & 2 & -1 & 0 \\ 0 & -1 & 2 & -1 \\ 0 & 0 & -1 & 1 \end{bmatrix}, \quad B^z = \begin{bmatrix} 1 & 0 & 0 & 0 \\ 0 & 0 & 0 & 0 \\ 0 & 0 & 0 & 0 \\ 0 & 0 & 0 & 1 \end{bmatrix},$$

$$L^v = \begin{bmatrix} 1 & 0 & 0 & -1 \\ 0 & 1 & -1 & 0 \\ 0 & -1 & 2 & -1 \\ -1 & 0 & -1 & 2 \end{bmatrix}, \quad B^v = \begin{bmatrix} 1 & 0 & 0 & 0 \\ 0 & 1 & 0 & 0 \\ 0 & 0 & 0 & 0 \\ 0 & 0 & 0 & 0 \end{bmatrix},$$

$$L^a = \begin{bmatrix} 1 & -1 & 0 & 0 \\ -1 & 2 & -1 & 0 \\ 0 & 0 & 1 & -1 \\ 0 & -1 & -1 & 2 \end{bmatrix}, \quad B^a = \begin{bmatrix} 1 & 0 & 0 & 0 \\ 0 & 0 & 0 & 0 \\ 0 & 0 & 1 & 0 \\ 0 & 0 & 0 & 0 \end{bmatrix},$$

The other parameters are chosen as $\lambda_v = 1$, $\lambda_a = 1$, $\iota = 0.35$, $h = 0.01$, $\bar{\varsigma} = 0.06$, $\gamma = 0.002$, $\tau_M = 0.02$, $r = 12$, and $\mu = 0.6$. The deception attack is considered as $f(x(t)) = -\tanh(0.2x(t))$.

Choose the initial states of the follower vehicles in the autonomous motorcade as $x_1(0) = [75, 24, 0]^T$, $x_2(0) = [50, 21, 0]^T$, $x_3(0) = [26, 18, 0]^T$, $x_4(0) = [3, 15, 0]^T$, where $x_0(0) = [100, 20, 0]^T$, and $\omega_i(t) = [0.5e^{-0.2t}\sin(t), 0.5e^{-0.2t}\sin(t), 0]$.

To verify the effectiveness and superiority of the proposed HT-based ETM, the following four cases are presented.

Case 1: The AMS with deception attacks using the proposed HT-based event-triggered control strategy.

Based on the above parameter selection, the event-triggered matrices Ω_i and controller gain K are obtained from Theorem 2 as follows:

$$K = \begin{bmatrix} 0.0673 & 0.0611 & -0.0371 \end{bmatrix},$$

$$\Omega_1 = \begin{bmatrix} 0.3920 & 0.3047 & -0.2677 \\ 0.3047 & 1.0910 & -0.3710 \\ -0.2677 & -0.3710 & 0.6505 \end{bmatrix},$$

$$\Omega_2 = \begin{bmatrix} 0.2918 & 0.2791 & -0.2402 \\ 0.2791 & 1.0698 & -0.3881 \\ -0.2402 & -0.3881 & 1.0792 \end{bmatrix},$$

$$\Omega_3 = \begin{bmatrix} 0.2574 & 0.1846 & -0.2305 \\ 0.1846 & 0.6339 & -0.3536 \\ -0.2305 & -0.3536 & 1.0616 \end{bmatrix},$$

$$\Omega_4 = \begin{bmatrix} 0.3996 & 0.3062 & -0.2621 \\ 0.3062 & 0.7313 & -0.3368 \\ -0.2621 & -0.3368 & 0.6263 \end{bmatrix}.$$

The distances between the leader vehicle and each follower vehicle in the motorcade are illustrated in Fig. 3, from which one can see that each vehicle maintains a distance, ensuring the safety of autonomous motorcade. Fig. 4 depicts the speed

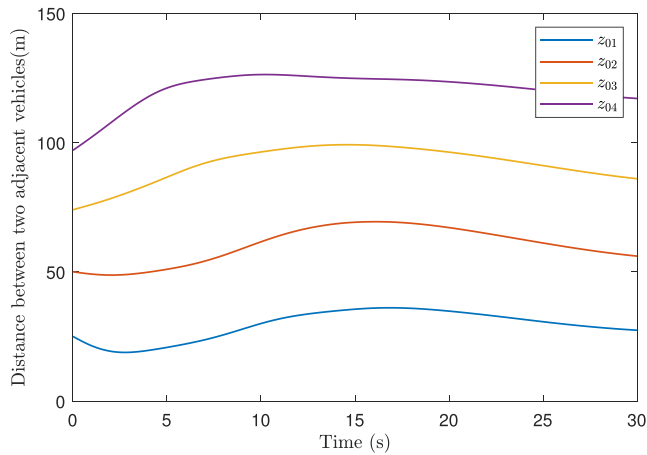


Fig. 3. Distances between the lead vehicle and follower vehicles in Case 1.

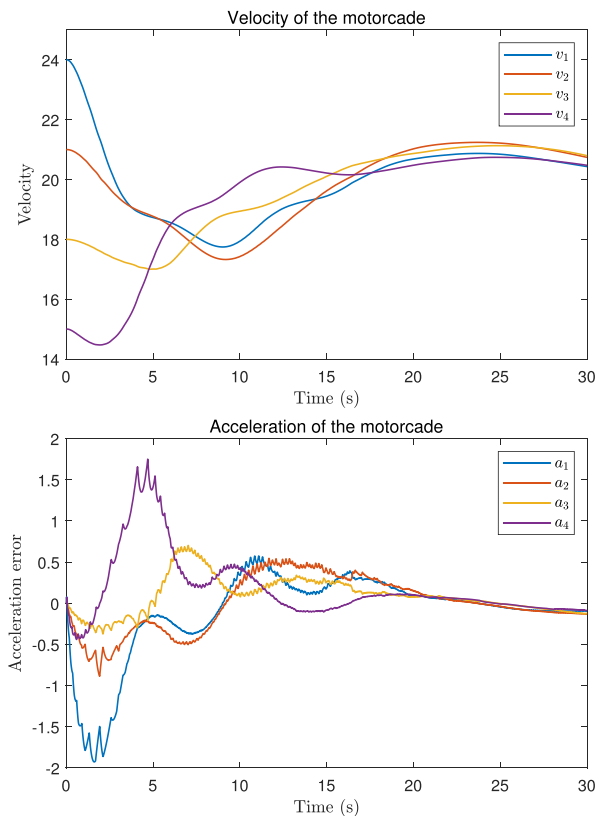


Fig. 4. Velocity and acceleration error in Case 1.

and acceleration responses of the following vehicles in the autonomous motorcade. It is evident that under the HT-based event-triggered control strategy proposed in this study, the velocities and accelerations of the vehicles with varying initial states in the motorcade are effectively stabilized.

Fig. 5 presents the data release instants of the AMS under the HT-based ETM. The corresponding data release rates are detailed in Table I, the average data release rate of each agent in the motorcade is 18.82%, significantly saving network resources. Therefore, the proposed HT-based ETM achieves more

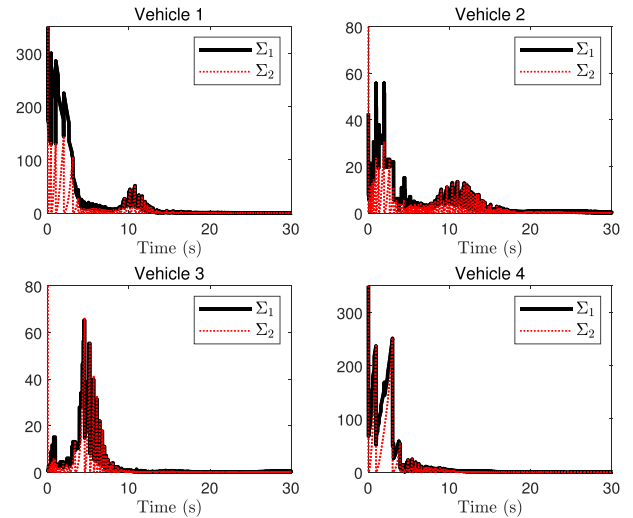

 Fig. 5. Release instants of the i -th vehicle in Case 1.

 TABLE I
 DATE RELEASE RATES OF THE FOLLOWER VEHICLES IN CASES 1 AND 2

	1	2	3	4
Case 1	18.16%	13.93%	21.13%	22.07%
Case 2	18.03%	9.13%	21.70%	20.47%

satisfactory consensus control with less resource consumption when AMS is subject to deception attacks.

Case 2: The AMS with deception attacks under partial disconnection of inter-vehicle communication.

In this case, the communication between the 2-nd and 3-rd vehicles is assumed to be severed in the motorcade due to network malfunction as illustrated in Remark 6. As shown in Fig. 2, within the positional network topology, these vehicles were previously directly linked, whereas in the velocity topology, the 2-nd vehicle remained directly connected to the root node, with the 3-rd vehicle linked indirectly.

Under identical initial conditions and a deception attack, the disconnection between the 2-nd and 3-rd vehicles requires the recalculation of the controller gain K and the triggering matrices Ω_i . The solutions for these parameters are derived as follows:

$$K = \begin{bmatrix} 0.0687 & 0.0785 & -0.0456 \end{bmatrix},$$

$$\Omega_1 = \begin{bmatrix} 0.6999 & 1.3467 & -0.6320 \\ 1.3467 & 10.2683 & -1.9453 \\ -0.6320 & -1.9453 & 2.4335 \end{bmatrix},$$

$$\Omega_2 = \begin{bmatrix} 0.6017 & 2.8494 & -0.7473 \\ 2.8494 & 26.2966 & -4.3110 \\ -0.7473 & -4.3110 & 4.4306 \end{bmatrix},$$

$$\Omega_3 = \begin{bmatrix} 0.3490 & 0.6595 & -0.5246 \\ 0.6595 & 4.5926 & -1.8423 \\ -0.5246 & -1.8423 & 4.0635 \end{bmatrix},$$

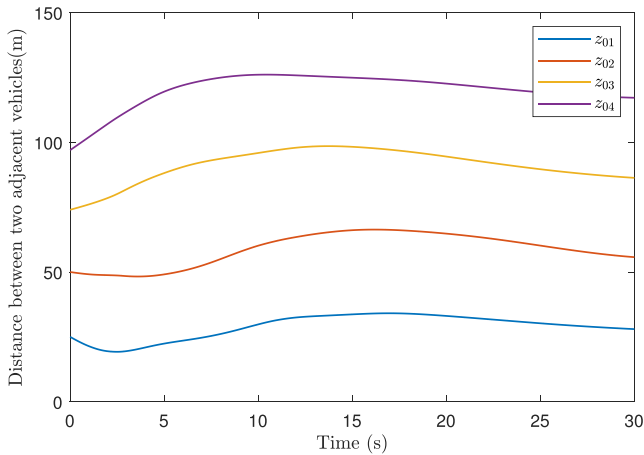


Fig. 6. Distances between the leader vehicle and follower vehicles in Case 2.

$$\Omega_4 = \begin{bmatrix} 0.6457 & 1.1052 & -0.5573 \\ 1.1052 & 5.2702 & -1.6308 \\ -0.5573 & -1.6308 & 2.2835 \end{bmatrix}.$$

Fig. 6 shows the distance between the leader vehicle and each follower vehicle in the autonomous motorcade when the connection between the 2nd and 3rd vehicles is disrupted under the deception attack. It is evident that the distances between each vehicle and its adjacent ones still comply with a safety level. Furthermore, compared to Fig. 3, there is no significant change in the settling time for vehicle spacing.

Fig. 7 shows the velocity and acceleration in the HT motorcade where disconnection occurs. Comparing Fig. 7 with Fig. 4 reveals that the disconnection of inter-vehicle connectivity under HT-based event-triggered control has little effect on the stable travel of the motorcade. Meanwhile, the convergence rates of velocity and acceleration remain almost the same. However, the amplitudes in the acceleration of the following vehicles are more noticeable, which is attributed to the disconnection of connectivity under the deception attack. Nevertheless, these results are within an acceptable range. Further verification will be conducted in Case 3.

The data release instants of the HT-based ETM in Case 2 are shown in Fig. 8. From Figs. 5 and 8, it is evident that under the proposed HT-based ETM, the effect of vehicle disconnection on the number of packet releases is minimal. Observing Y-axis between Figs. 5 and 8 reveals that the significant difference in both cases. Our primary focus is on whether the quasi-relative error can trigger the release event, which is more critical for evaluating the effectiveness of the event-trigger mechanism.

The data release instants of the HT-based ETM in Case 2 are illustrated in Fig. 8. From Figs. 5 and 8, and Table I, it is evident that under the proposed HT-based ETM, the impact of vehicle disconnection on the number of packet releases has no significant difference. Examining the Y-axis values in Figs. 5 and 8 reveals noticeable discrepancies. However, the main focus is to determine whether the quasi-relative error can trigger the release event, which is crucial for assessing the effectiveness of the event-triggering mechanism. This demonstrates that the

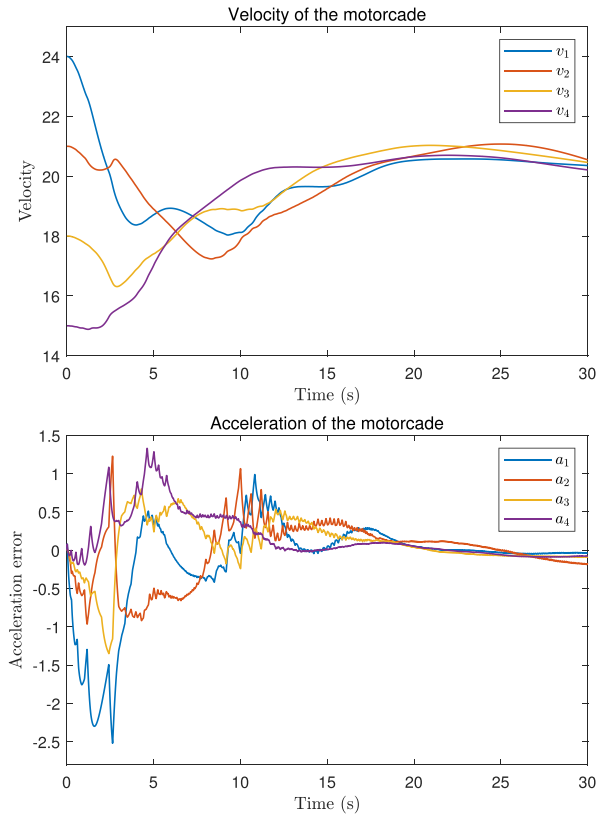


Fig. 7. Velocity and acceleration error in Case 2.

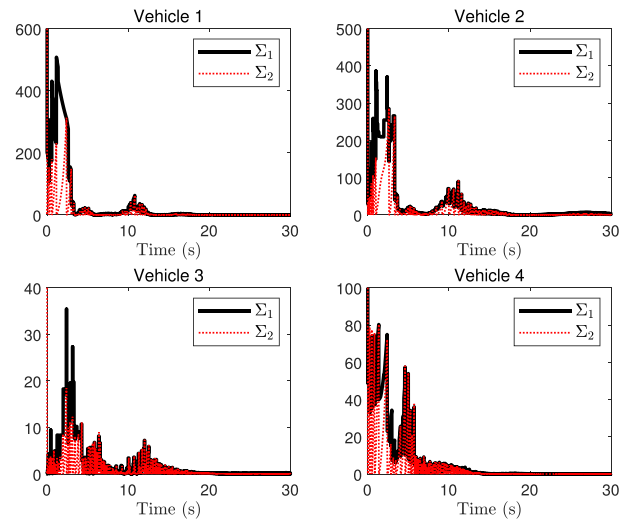


Fig. 8. Release instants of the i -th vehicle in Case 2.

HT-based event-triggered control strategy for AMS maintains consensus performance even when some inter-vehicle connections are disrupted.

Table I presents the data release rates of the AMS in Cases 1 and 2. The average rates are 18.82% and 17.33%, indicating that 81.18% and 82.67% of the sampled data are discarded, respectively. This reduction significantly conserves network communication resources. Despite the high rate of data discarding, consensus control in both cases maintains good performance.

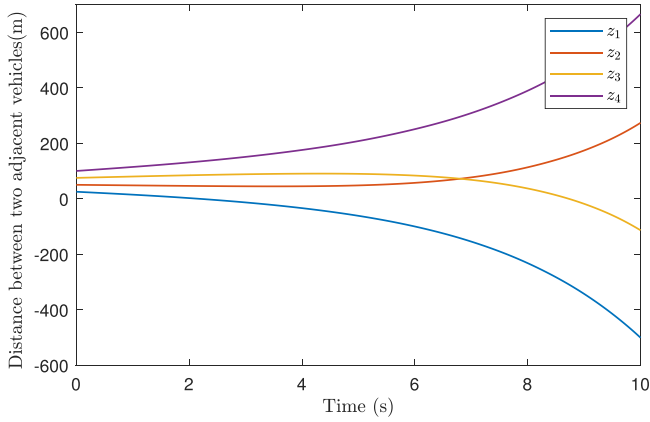


Fig. 9. Distances between the leader vehicle and the follower vehicles in Case 3.

To further verify the superiority of the HT-based event-triggered control strategy over the INT-based ETM strategy, a motorcade with an INT was established for comparison. As mentioned in Corollary 1, the degree matrix and the adjacency matrix are equivalent to L^z and B^z when the positions, velocities, and accelerations of the autonomous motorcade interact with each other using the topology shown in Fig. 2.

Case 3: The AMS with deception attacks using an INT-based event-triggered control strategy.

In this case, we suppose the communication in the AMS is interrupted due to deception attacks, and an INT is utilized as that in [5], [9]. Then H is rewritten by

$$H^z = \begin{bmatrix} 2 & -1 & 0 & 0 \\ -1 & 2 & -1 & 0 \\ 0 & -1 & 2 & -1 \\ 0 & 0 & -1 & 2 \end{bmatrix}.$$

From Corollary 1, the parameters of K and Ω_i ($i = 1, 2, 3, 4$) can be obtained. Under the same conditions as Case 2, the distances between the follower vehicles and the leader vehicle in the motorcade with the INT are shown in Fig. 9. The velocity and acceleration responses of each vehicle under the traditional INT-based control strategy are illustrated in Fig. 10. It is evident that the AMS with INT, as described in [5], [9], fails to maintain consensus stability when the AMS is disconnected due to deception attacks. Comparing to Case 2, our proposed HT-based ETM demonstrates superior robustness in achieving consensus control of the AMS.

In Cases 1-3, 4 vehicles have been used to demonstrated the effectiveness of the proposed method. To further validate its applicability to larger-scale scenarios, the following analysis will consider more follower vehicles.

Case 4: Larger-scale AMS with one leader vehicle and five followers using the proposed HT-based event-triggered control strategy.

Assume that the AMS consists of one leader vehicle and five follower vehicles and the topological relationships of the position, velocity, and acceleration are illustrated in Fig. 11. Based on these topological relationships, the relevant parameters

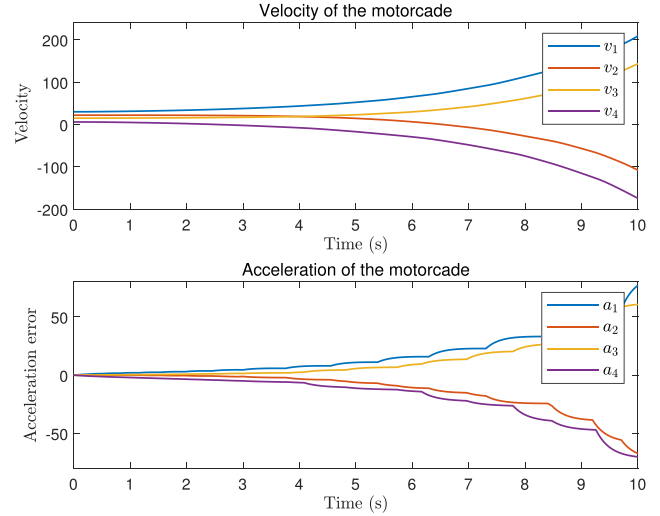


Fig. 10. Velocity and acceleration error in Case 3.

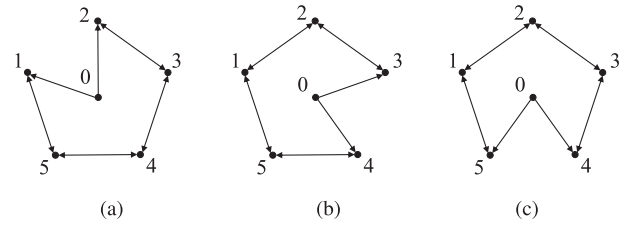


Fig. 11. The topology graph of PVA in Case 4. (a) Position. (b) Velocity. (c) Acceleration.

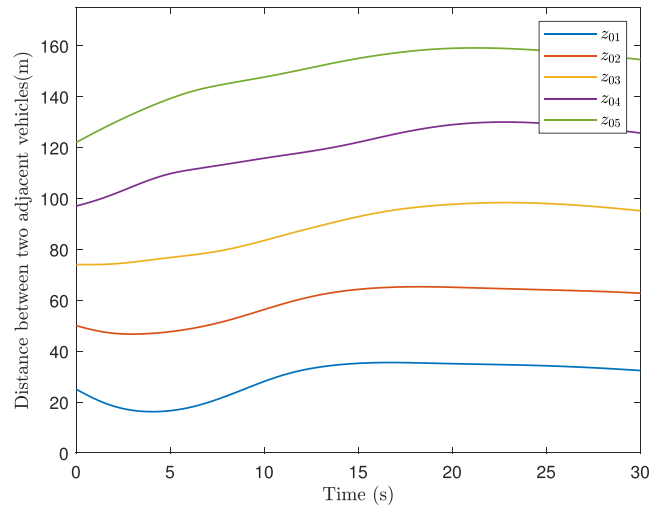


Fig. 12. Distances between the leader vehicle and the follower vehicles in Case 4.

can be obtained from Theorem 2 with the same parameters as those in Case 1.

The initial states of the follower vehicles are assumed to be $x_1(0) = [75, 24, 0]^T$, $x_2(0) = [50, 22, 0]^T$, $x_3(0) = [26, 20, 0]^T$, $x_4(0) = [3, 18, 0]^T$, and $x_5(0) = [-22, 16, 0]^T$, and the leader vehicle's initial state is $x_0(0) = [100, 20, 0]^T$. Fig. 12 shows the distances between the leader and follower

vehicles, demonstrating that the AMS with five follower vehicles maintains satisfactory performance under the proposed HT-based ETM.

V. CONCLUSION

In this paper, the HT-based event-triggered consensus control of AMS under deception attacks has been investigated. A new HT-based ETM that introduces vehicle position, velocity, and acceleration is designed, along with a reorganization matrix that effectively addresses Kronecker product misalignment. Due to the introduction of a more fully connected topology, the proposed HT-based event-triggered control strategy demonstrates better robustness compared to traditional INT-based motorcades. The HT-based AMS remains stable and low data release rates even when certain vehicles are disconnected or subjected to deception attacks. The advantages of the proposed control strategy are verified in an AMS consisting of a leader vehicle and four follower vehicles.

REFERENCES

- [1] J. Wang, C. Jiang, Z. Han, Y. Ren, and L. Hanzo, "Internet of vehicles: Sensing-aided transportation information collection and diffusion," *IEEE Trans. Veh. Technol.*, vol. 67, no. 5, pp. 3813–3825, May 2018.
- [2] C. Yang, B. Liu, H. Li, B. Li, K. Xie, and S. Xie, "Learning based channel allocation and task offloading in temporary UAV-assisted vehicular edge computing networks," *IEEE Trans. Veh. Technol.*, vol. 71, no. 9, pp. 9884–9895, Sep. 2022.
- [3] Z. Gu, X. Huang, X. Sun, X. Xie, and J. H. Park, "Memory-event-triggered tracking control for intelligent vehicle transportation systems: A leader-following approach," *IEEE Trans. Intell. Transp. Syst.*, vol. 25, no. 5, pp. 743–752, May, 2024.
- [4] S. Chen, J. Dong, P. Ha, Y. Li, and S. Labi, "Graph neural network and reinforcement learning for multi-agent cooperative control of connected autonomous vehicles," *Comput.-Aided Civil Infrastructure Eng.*, vol. 36, no. 7, pp. 838–857, 2021.
- [5] G. Wu, G. Chen, H. Zhang, and C. Huang, "Fully distributed event-triggered vehicular platooning with actuator uncertainties," *IEEE Trans. Veh. Technol.*, vol. 70, no. 7, pp. 6601–6612, Jul. 2021.
- [6] V. S. Dolk, J. Ploeg, and W. M. H. Heemels, "Event-triggered control for string-stable vehicle platooning," *IEEE Trans. Intell. Transp. Syst.*, vol. 18, no. 12, pp. 3486–3500, Dec. 2017.
- [7] W. He, B. Xu, Q. L. Han, and F. Qian, "Adaptive consensus control of linear multiagent systems with dynamic event-triggered strategies," *IEEE Trans. Cybern.*, vol. 50, no. 7, pp. 2996–3008, Jul. 2020.
- [8] W. Hu, C. Yang, T. Huang, and W. Gui, "A distributed dynamic event-triggered control approach to consensus of linear multiagent systems with directed networks," *IEEE Trans. Cybern.*, vol. 50, no. 2, pp. 869–874, Feb. 2020.
- [9] D. Zhang, Y. P. Shen, S. Q. Zhou, X. W. Dong, and L. Yu, "Distributed secure platoon control of connected vehicles subject to DoS attack: Theory and application," *IEEE Trans. Syst., Man, Cybern. Syst.*, vol. 51, no. 11, pp. 7269–7278, Nov. 2021.
- [10] Y. Y. Qian, L. Liu, and G. Feng, "Distributed event-triggered adaptive control for consensus of linear multi-agent systems with external disturbances," *IEEE Trans. Cybern.*, vol. 50, no. 5, pp. 2197–2208, May 2020.
- [11] A. Joshi, "Review of vehicle engine efficiency and emissions," *SAE Int. J. Adv. Curr. Practices Mobility*, vol. 1, pp. 734–761, 2019.
- [12] E. Panteley and A. Loria, "Synchronization and dynamic consensus of heterogeneous networked systems," *IEEE Trans. Autom. Control*, vol. 62, no. 8, pp. 3758–3773, Aug. 2017.
- [13] Y. Y. Qian, L. Liu, and G. Feng, "Output consensus of heterogeneous linear multi-agent systems with adaptive event-triggered control," *IEEE Trans. Autom. Control*, vol. 64, no. 6, pp. 2606–2613, Jun. 2019.
- [14] W. Zhengxin and H. Haibo, "Asynchronous quasi-consensus of heterogeneous multiagent systems with nonuniform input delays," *IEEE Trans. Syst., Man, Cybern. Syst.*, vol. 50, no. 8, pp. 2815–2827, Aug. 2020.
- [15] B. Cheng and Z. Li, "Coordinated tracking control with asynchronous edge-based event-triggered communications," *IEEE Trans. Autom. Control*, vol. 64, no. 10, pp. 4321–4328, Oct. 2019.
- [16] C. Wang, D. Wang, and Z. Peng, "Distributed output-feedback control of unmanned container transporter platooning with uncertainties and disturbances using event-triggered mechanism," *IEEE Trans. Veh. Technol.*, vol. 71, no. 1, pp. 162–170, Jan. 2022.
- [17] F. Gao, X. Hu, S. E. Li, K. Li, and Q. Sun, "Distributed adaptive sliding mode control of vehicular platoon with uncertain interaction topology," *IEEE Trans. Ind. Electron.*, vol. 65, no. 8, pp. 6352–6361, Aug. 2018.
- [18] Z. Gu, Y. Fan, T. Yin, and S. Yan, "A novel event-triggered load frequency control for power systems with electric vehicle integration," *IEEE Trans. Syst., Man, Cybern.: Syst.*, early access, Oct. 30, 2024, doi: [10.1109/TSMC.2024.3485164](https://doi.org/10.1109/TSMC.2024.3485164).
- [19] K. Yu, Y. Li, Z. Peng, and S. Tong, "Distributed event-triggered formation control of planar vehicles without velocity sensors," *IEEE Trans. Veh. Technol.*, vol. 72, no. 3, pp. 2988–3000, Mar. 2023.
- [20] Z. Gu, P. Shi, D. Yue, and Z. Ding, "Decentralized adaptive event-triggered H_∞ filtering for a class of networked nonlinear interconnected systems," *IEEE Trans. Cybern.*, vol. 49, no. 5, pp. 1570–1579, May 2019.
- [21] R. Xu, X. Wang, and Y. Zhou, "Observer-based event-triggered adaptive containment control for multiagent systems with prescribed performance," *Nonlinear Dyn.*, vol. 107, no. 3, pp. 2345–2362, 2022.
- [22] Z. Li, B. Hu, M. Li, and G. Luo, "String stability analysis for vehicle platooning under unreliable communication links with event-triggered strategy," *IEEE Trans. Veh. Technol.*, vol. 68, no. 3, pp. 2152–2164, Mar. 2019.
- [23] S. Hu, J. Qiu, X. Chen, F. Zhao, and X. Jiang, "Dynamic event-triggered control for leader-following consensus of multiagent systems with the estimator," *IET Control Theory Appl.*, vol. 16, pp. 475–484, 2022.
- [24] Z. Cheng, D. Yue, S. Hu, H. Ge, and L. Chen, "Distributed event-triggered consensus of multi-agent systems under periodic DoS jamming attacks," *Neurocomputing*, vol. 400, pp. 458–466, 2020.
- [25] N. Zhao, X. Zhao, M. Chen, G. Zong, and H. Zhang, "Resilient distributed event-triggered platooning control of connected vehicles under denial-of-service attacks," *IEEE Trans. Intell. Transp. Syst.*, vol. 24, no. 6, pp. 6191–6202, Jun. 2023, doi: [10.1109/TITS.2023.3250402](https://doi.org/10.1109/TITS.2023.3250402).
- [26] J. Wang, D. Wang, L. Su, J. H. Park, and H. Shen, "Dynamic event-triggered H_∞ load frequency control for multi-area power systems subject to hybrid cyber attacks," *IEEE Trans. Syst., Man, Cybern. Syst.*, vol. 52, no. 12, pp. 7787–7798, Dec. 2022.
- [27] T. Yin, Z. Gu, and J. H. Park, "Event-based intermittent formation control of multi-UAV systems under deception attacks," *IEEE Trans. Neural Netw. Learn. Syst.*, vol. 35, no. 6, pp. 8336–8347, Dec. 2022, doi: [10.1109/TNNLS.2022.3227101](https://doi.org/10.1109/TNNLS.2022.3227101).
- [28] H.-T. Sun and C. Peng, "Event-triggered adaptive security path following control for unmanned ground vehicles under sensor attacks," *IEEE Trans. Veh. Technol.*, vol. 72, no. 7, pp. 8500–8509, Jul. 2023, doi: [10.1109/TVT.2023.3250709](https://doi.org/10.1109/TVT.2023.3250709).
- [29] Z. Gu, T. Yin, and Z. Ding, "Path tracking control of autonomous vehicles subject to deception attacks via a learning-based event-triggered mechanism," *IEEE Trans. Neural Netw. Learn. Syst.*, vol. 32, no. 12, pp. 5644–5653, Dec. 2021.
- [30] X. Mu, Z. Gu, and Q. Lu, "Memory-event-triggered consensus control for multi-UAV systems against deception attacks," *ISA Trans.*, vol. 32, no. 12, pp. 5644–5653, Dec. 2021, doi: [10.1016/j.isatra.2023.04.028](https://doi.org/10.1016/j.isatra.2023.04.028).
- [31] S. Xiao, X. Ge, Q. L. Han, Z. Cao, and H. Wang, "Resilient distributed event-triggered control of vehicle platooning under DoS attacks," *IFAC-PapersOnLine*, vol. 53, no. 2, pp. 1807–1812, 2020.
- [32] S. Wen and G. Guo, "Cooperative control and communication of connected vehicles considering packet dropping rate," *Int. J. Syst. Sci.*, vol. 49, no. 13, pp. 2808–2825, 2018.
- [33] S. Wen, G. Guo, B. Chen, and X. Gao, "Cooperative adaptive cruise control of vehicles using a resource-efficient communication mechanism," *IEEE Trans. Intell. Veh.*, vol. 4, no. 1, pp. 127–140, Mar. 2019.
- [34] T. G. Molnár, W. B. Qin, T. Insperger, and G. Orosz, "Application of predictor feedback to compensate time delays in connected cruise control," *IEEE Trans. Intell. Transp. Syst.*, vol. 19, no. 2, pp. 545–559, Feb. 2018.
- [35] É. Gyurkovics, "A note on Wirtinger-type integral inequalities for time-delay systems," *Automatica*, vol. 61, pp. 44–46, 2015.